Active Role of a Germylene Ligand in Promoting Reactions of Platinum Complexes with Oxygen and Sulfur Dioxide

K. E. Litz, M. M. Banaszak Holl,* J. W. Kampf, and G. B. Carpenter[†]

Department of Chemistry, The University of Michigan, Ann Arbor, Michigan 48109-1055

Received July 13, 1998

The reaction of $(Et_3P)_2PtGe[N(SiMe_3)_2]_2$ with dioxygen yields $(Et_3P)_2Pt(\mu\text{-}\eta^2\text{-}O_2)Ge[N(SiMe_3)_2]_2$ (**1**). Exposure of **1** to light resulted in a rearrangement to $(Et_3P)_2PtO_2Ge[N(SiMe_3)_2]_2$ (**2a**), the first example of a bidentate, dianionic germanate ligand. The isomerization was judged to occur via an intramolecular O−O bond scission and rotation of the Pt−Ge bond. No free germylene was detected, and the reaction was found to be zero order. An analogue of **2a** was prepared by direct reaction of $(Ph_3P)_2PtO_2$ with $Ge[N(SiMe_3)_2]_2$ yielding $(Ph_3P)_2PtO_2$-$Ge[N(SiMe_3)_2]_2$ (**2b**). Addition of SO_2 to **1** results in the formation of the bridging sulfate $(Et_3P)_2Pt(\mu\text{-}\eta^2\text{-}SO_4)$-$Ge[N(SiMe_3)_2]_2$ (**3**). An infrared spectroscopy study of the sulfate reaction was performed using oxygen-18. The results indicate that direct insertion of SO_2 into the O−O bond does not occur. Formaldehyde was also observed to insert into the Pt−O bond of **1** giving $(Et_3P)_2Pt(\mu\text{-}\eta^2\text{-}OCH_2OO)Ge[N(SiMe_3)_2]_2$ (**5**).

Introduction

Oxidation of low-valent organometallic complexes and transition metal catalysts by molecular oxygen is a field of both academic and industrial importance for several reasons. Metal peroxo complexes are believed to be important intermediates in the Pt-catalyzed synthesis of sulfuric acid and are thought to precede the partial oxidation of saturated and unsaturated hydrocarbons by transition metal catalysts.[1] Metal peroxo complexes also play a role in the uptake and utilization of dioxygen by biological and biomimetic transition-metal complexes.[2] Oxygen is also known to poison catalysts and degrade organotransition metal compounds.[3] The many ways that oxygen can interact with metal complexes are underscored by the wide variety of coordination modes displayed in Chart 1.

Many dioxygen complexes have been observed to react with SO_2 yielding metal sulfate adducts.[4,5] The first studies with group 10 metals, which included synthesis of $(Ph_3P)_2PtO_2$ and subsequent reaction with SO_2 to form the bound sulfate (eq 1),

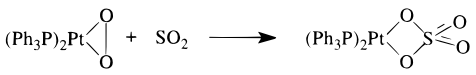

(1)

Chart 1. Common Coordination Modes of Dioxygen

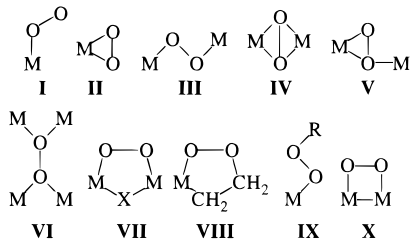

were reported approximately 30 years ago.[6] The first bimetallic type X peroxo complex containing two transition metals, $[Ir_2I_2(CO)_2(\mu\text{-}\eta^2\text{-}O_2)(dppm)_2]_2$, was published by Cowie et al. in 1990.[7] This compound was unique in having a peroxo moiety bridging a metal−metal bond. All previous bridging peroxo groups had been of types III−VII. Cowie's bridging peroxide also forms a bound sulfate in the presence of SO_2 (eq 2). Main

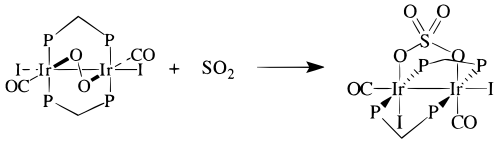

(2)

group type X peroxo complexes are known for digermenes and disilenes; however, their reactivity with SO_2 has not been reported.[8,9] As part of a general study of germylenes as "active" ligands for transition metals, we explored the reactivity of $(Et_3P)_2PtGe[N(SiMe_3)_2]_2$ with dioxygen. The germylene ligand

[†] Department of Chemistry, Brown University, Providence, RI 02912.

(1) Thorough reviews of this subject can be found in the following: (a) Sheldon, R. A.; Kochi, J. K. *Metal-Catalyzed Oxidation of Organic Compounds*; Academic Press: New York, 1981. (b) Pines, H. *The Chemistry of Catalytic Hydrocarbon Conversion*; Academic Press: New York, 1981; pp 213−230. (c) Shilov, A. E. *Catalysis by Metal Complexes: Activation of Saturated Hydrocarbons by Transition Metal Complexes*; D. Reidel Publishing: Boston, MA, 1984; pp 62−141. (d) Jorgensen, K. A. *Chem. Rev.* **1989**, *89*, 431. (e) Simandi, L. I. *Catalysis By Metal Complexes: Catalytic Activation of Dioxygen by Metal Complexes*; Kluwer Academic Publishers: Boston, MA, 1992.

(2) Selected reviews can be found in the following: (a) Martell, A. E.; Sawyer, D. T. *Oxygen Complexes and Oxygen Activation by Transition Metals*; Plenum: New York, 1988. (b) Tyeklar, Z.; Karlin, K. D. *Acc. Chem. Res.* **1989**, *22*, 241. (c) Sawyer, D. T., Ed. *Oxygen Chemistry*; Oxford University Press: New York, 1991. (d) Lippard, S. J.; Berg, J. M. *Principles of Bioinorganic Chemistry*; University Science Books: Mill Valley, CA, 1994.

(3) Hegedus, L. L.; McCabe, R. W. *Catalyst Poisoning*; Marcel Dekker Inc.: New York, 1984.

(4) Valentine, J. S. *Chem. Rev.* **1973**, *73*, 235.

(5) Kubas, G. J. *Acc. Chem. Res.* **1994**, *27*, 183.

(6) (a) Takahasi, S.; Sonogashira, K.; Hagihara, N. *J. Chem. Soc. Jpn.* **1966**, *87*, 610. (b) Wilke, G.; Shott, H.; Heimbach, P. *Angew. Chem., Int. Ed. Engl.* **1967**, *6*, 92. (c) Cook, C. D.; Jauhal, G. S. *Inorg. Nucl. Chem. Lett.* **1967**, *3*, 31.

(7) (a) Xiao, J.; Santarsiero, B. D.; Vaartstra, B. A.; Cowie, M. *J. Am. Chem. Soc.* **1993**, *115*, 3212. (b) Vaartstra, B. A.; Xiao, J.; Cowie, M. *J. Am. Chem. Soc.* **1990**, *112*, 9425.

(8) Masamune, S.; Batcheller, S. A.; Park, J.; Davis, W. M. *J. Am. Chem. Soc.* **1989**, *111*, 1888.

(9) (a) Michalczyk, M. J.; West, R.; Michl, J. *J. Chem. Soc., Chem. Commun.* **1984**, 1525. (b) Fink, M. J.; De Young, D. J.; West, R.; Michl, J. *J. Am. Chem. Soc.* **1983**, *105*, 1070. (c) Fink, M. J.; Haller, K. J.; West, R.; Michl, J. *J. Am. Chem. Soc.* **1984**, *106*, 822.

10.1021/ic9808044 CCC: $15.00
Published on Web 11/19/1998

was found to cooperate in an intimate fashion with the central platinum center in the binding of O_2. Given the recent precedence for reversible germanium−oxygen bond formation,[10,11] we anticipated that this system might allow for reversible binding of O_2 and/or the reaction products of the metal peroxo complexes.

In this paper, we report the synthesis and characterization of the first mixed transition-metal/main-group peroxo complex, $(Et_3P)_2Pt(\mu\text{-}\eta^2\text{-}O_2)Ge[N(SiMe_3)_2]_2$ (**1**). Complex **1** photochemically rearranges to $(Et_3P)_2PtO_2Ge[N(SiMe_3)_2]_2$ (**2a**), a complex containing a unique bidentate germanate ligand. In addition, **1** undergoes reaction with SO_2 and $H_2C{=}O$ leading to the bridging adducts $(Et_3P)_2Pt(\mu\text{-}\eta^2\text{-}SO_4)Ge[N(SiMe_3)_2]_2$ (**3**) and $(Et_3P)_2Pt(\mu\text{-}\eta^2\text{-}OCH_2OO)Ge[N(SiMe_3)_2]_2$ (**5**), respectively. The mechanism of sulfate formation was probed using $^{18}O_2$ labeling experiments and infrared spectroscopy. Reduction of **3** with Na/Hg amalgam regenerated $(Et_3P)_2PtGe[N(SiMe_3)_2]_2$. The activation of dioxygen, its conversion to sulfate, and facile removal demonstrate a complete stepwise cycle for the conversion of SO_2 to $[SO_4]^{2-}$.

Experimental Section

All manipulations were performed using air-free techniques and dry, deoxygenated solvents unless otherwise stated. $(Et_3P)_2PtGe[N(SiMe_3)_2]_2$,[11a] $(Ph_3P)_2PtO_2$,[12] $(Et_3P)_2PtCO_3$,[13] and $Ge[N(SiMe_3)_2]_2$[14] were prepared according to published procedures. Oxygen (99.6%) and benzil were utilized as received from Aldrich Chemical. Anhydrous sulfur dioxide was used as received from Matheson Gas Products. Benzene-d_6, benzene, diethyl ether, THF, and pentane solvents were all degassed and distilled over sodium benzophenone ketyl. Acetonitrile was degassed, dried by refluxing over P_2O_5, and distilled onto activated 4 Å molecular sieves. The 95% $^{18}O_2$ was obtained from Icon Services. All other reagents were used as received from Aldrich Chemical. IR spectra were obtained on a Nicolet 5DXB FT-IR or a Bio-Rad FTS40 FT-IR as NaCl/Nujol mulls or as pressed KBr or CsI pellets. ^{1}H, ^{13}C, and ^{31}P NMR spectra were obtained in the listed deuterated solvents on a Bruker AM-360 spectrometer (360.1, 90.6, and 145.8 MHz) and referenced to residual protons, solvent carbons, and external 85% H_3PO_4 in D_2O, respectively. Microanalyses were performed by University of Michigan Analytical Services.

$(Et_3P)_2Pt(\mu\text{-}\eta^2\text{-}O_2)Ge[N(SiMe_3)_2]_2$ (1). A hexane solution containing 400 mg (0.48 mmol) of $(Et_3P)_2PtGe[N(SiMe_3)_2]_2$ was stirred, blanketed with 1 atm of O_2, and protected from light. The initially golden yellow solution developed a light green hue after 20 min. An aliquot analyzed by ^{1}H NMR revealed quantitative conversion to **1**. The solvent volume was reduced to one-third. The product was isolated by cold filtration on a fritted glass filter disk as a bright yellow-green solid (272 mg, 66% yield). **1** was observed to be moisture and light sensitive: ^{1}H NMR (C_6D_6) δ 0.69 (s, 36 H, Si(CH_3)$_3$), 0.82 (m, 18 H, CH_2CH_3), 1.34 (m, 6 H, CH_2CH$_3$), 1.55 (m, 6 H, CH_2CH$_3$); ^{13}C{^{1}H} NMR (C_6D_6) δ 21.2 (m, *C*H_2CH$_3$), 14.8 (m, *C*H_2CH$_3$), 9.5 (m, CH_2CH_3), 8.3 (m, CH_2CH_3), 7.4 (s, Si(*C*H$_3$)$_3$); ^{31}P{^{1}H} NMR (C_6D_6) δ 16.2 (d, w/^{195}Pt satellites, $^1J_{Pt-P}$ = 1839 Hz, $^2J_{P-P}$ = 10.6 Hz), −5.3 (d w/^{195}Pt satellites, $^1J_{Pt-P}$ = 3125 Hz, $^2J_{P-P}$ 10.3 Hz). Anal. Calcd for $C_{24}H_{66}GeN_2O_2P_2PtSi_4$: C, 33.65; H, 7.76; N, 3.27. Found: C, 33.70; H, 7.43; N, 3.15.

$(Et_3P)_2PtO_2Ge[N(SiMe_3)_2]_2$ (2a). In a Pyrex bomb reactor, a 10 mL hexane solution containing 500 mg (0.61 mmol) $(Et_3P)_2PtGe[N(SiMe_3)_2]_2$ was stirred, blanketed with 1 atm O_2, and exposed to a 100 W Sylvania Par38 mercury lamp. After 10 min, the initially golden orange solution became olive colored. Hexane was removed *in vacuo* leaving a tan oil which crystallized upon standing for 24 h. Colorless crystals were obtained by washing with 1 mL of acetonitrile (307 mg, 59% yield): ^{1}H NMR (C_6D_6) δ 0.70 (s, 36 H, Si(CH_3)$_3$), 0.88 (m, 18 H, CH_2CH_3), 1.46 (m, 12 H, CH_2CH$_3$); ^{13}C NMR (C_6D_6) δ 15.8 (m, *C*H_2CH$_3$), 8.2 (m, CH_2CH_3), 6.6 (s, Si(*C*H$_3$)$_3$); ^{31}P{^{1}H} NMR (C_6D_6) δ 1.8 (s, w/^{195}Pt satellites, $^1J_{Pt-P}$ = 3284 Hz). Anal. Calcd for $C_{24}H_{66}GeN_2O_2P_2PtSi_4$: C, 33.65; H, 7.76; N, 3.27. Found: C, 33.73; H, 7.71; N, 3.23.

$(Ph_3P)_2PtO_2Ge[N(SiMe_3)_2]_2$ (2b). In a round-bottom flask protected from light by aluminum foil, a 5 mL ethereal solution of 1.8 g $(Ph_3P)_2PtO_2$ (2.39 mmol) and 0.943 g $Ge[N(SiMe_3)_2]_2$ was allowed to stir until all solids dissolved and the solution became dark orange-brown with formation of a white precipitate. After 1 h, all volatiles were removed *in vacuo*. The solids were washed with 2 × 5 mL pentane leaving 1.70 g (62% yield) off-white microcrystals: ^{1}H NMR (C_6D_6) δ 0.64 (s, 36 H, Si(CH_3)$_3$), 6.91 (m, 24 H, PPh_3), 7.69 (m, 6 H, PPh_3); ^{13}C-{^{1}H} NMR (C_6D_6) δ 6.15 (s, Si(*C*H$_3$)$_3$), 127.8 (d, phenyl), 128.1 (s, phenyl), 130.2 (s, phenyl), 135.1 (q, phenyl); ^{31}P{^{1}H} NMR (C_6D_6) δ 6.87 (s, w/^{195}Pt satellites, $^1J_{Pt-P}$ = 3461 Hz). Anal. Calcd for $C_{48}H_{66}GeN_2O_2P_2PtSi_4$: C, 50.35; H, 5.81; N, 2.45. Found: C, 50.47; H, 6.12; N, 2.43. IR (KBr pellet) (cm^{-1}): 3058 vs, 2952 s, 2896 s, 1483 m, 1434 s, 1349 m, 1279 s, 1244 vs, 1188 s, 1131 s, 1096 vs, 1033 w, 998 w, 913 vs, 864 vs, 843 vs, 745s, 688 vs, 527 vs. MS (CI, CH_4): 1146 amu, isotope distribution consistent with that calculated for $C_{48}H_{67}GeN_2O_2P_2PtSi_4$.

$(Et_3P)_2Pt(\mu\text{-}\eta^2\text{-}SO_4)Ge[N(SiMe_3)_2]_2$ (3). Complex **1** was generated *in situ* by allowing $(Et_3P)_2PtGe[N(SiMe_3)_2]_2$ (0.200 g 0.242 mmol) to react with 1 atm dioxygen for 25 min while protected from light. When the orange color faded, all volatiles were removed *in vacuo*, the solids were dissolved in toluene, and 1 atm of SO_2 was allowed to blanket the stirred solution for 2 h. The white solid that precipitated from solution was recovered by filtration and washed with hexane (0.120 g, 54% yield): ^{1}H NMR ($CDCl_3$) δ 0.35 (s, 36 H, Si(CH_3)$_3$), 1.16 (m, 18 H, CH_2CH_3), 1.98 (m, 6 H, CH_2CH$_3$), 2.10 (m, 6 H, CH_2CH$_3$); ^{13}C-{^{1}H} NMR ($CDCl_3$) δ 6.96 (s, $SiMe_3$), 8.45 (s, CH_2CH_3), 9.54 (s, CH_2CH_3), 14.60 (d, *C*H_2CH$_3$), 21.06 (d, *C*H_2CH$_3$); ^{31}P{^{1}H} NMR (C_6D_6) δ 21.7 (d, w/^{195}Pt satellites, $^1J_{Pt-P}$ = 1950 Hz, $^2J_{P-P}$ = 16.3 Hz), −7.6 (d w/^{195}Pt satellites, $^1J_{Pt-P}$ = 4020 Hz, $^2J_{P-P}$ = 17 Hz); IR (Nujol/NaCl) (cm^{-1}) 1283 s, 1153 s, 892 s. Anal. Calcd for $C_{24}H_{66}GeN_2O_2P_2PtSi_4$: C, 31.30; H, 7.22; N, 3.04. Found: C, 30.51; H, 6.96; N, 2.90.

$(Et_3P)_2Pt(\mu\text{-}\eta^2\text{-}OC(O)O)Ge[N(SiMe_3)_2]_2$ (4). A 5 mL THF solution containing 200 mg of $(Et_3P)_2PtCO_3$ and 160 mg of $Ge[N(SiMe_3)_2]_2$ was stirred for 2 h. The solvent was removed in vacuo. A white powder was recovered by filtration from pentane (211 mg, 59% yield): ^{1}H NMR ($CDCl_3$) δ 0.35 (s, 36H, Si(CH_3)$_3$), 1.12 (m, 18H, CH_2CH_3), 1.94 (m, 6H, CH_2CH$_3$), 2.02 (m, 6H, CH_2CH$_3$); ^{13}C{^{1}H} NMR ($CDCl_3$) δ 162.7 (d, *trans*-$^3J_{P-C}$ = 2.41 Hz, CO_3), 20.5 (m, *C*H_2CH$_3$), 14.6 (m, *C*H_2CH$_3$), 8.9 (m, CH_2CH_3), 7.9 (m, CH_2CH_3), 6.8 (s, Si(*C*H$_3$)$_3$); ^{31}P-{^{1}H} NMR ($CDCl_3$) δ 21.01 (d, w/^{195}Pt satellites, $^1J_{Pt-P}$ = 1934 Hz, $^2J_{P-P}$ = 17 Hz), −6.6 (d w/^{195}Pt satellites, $^1J_{Pt-P}$ = 3772 Hz, $^2J_{P-P}$ 17 Hz); IR (KBr) (cm^{-1}) 1652/1623 ν(C=O). Anal. Calcd for $C_{25}H_{66}GeN_2O_3P_2PtSi_4$: C, 33.94; H, 7.52; N, 3.17. Found: C, 33.93; H, 7.21; N, 2.96.

$(Et_3P)_2Pt(\mu\text{-}\eta^2\text{-}OCH_2OO)Ge[N(SiMe_3)_2]_2$ (5). THF was condensed into a 10 mL round-bottom two-neck flask charged with 0.200 g (0.24 mmol) $(Et_3P)_2PtGe[N(SiMe_3)_2]_2$, and the solution was allowed to stir under 1 atm O_2 for 1 h while protected from light. The volatiles were removed in vacuo to remove excess dioxygen. The contents were redissolved in THF, and 0.075 g of paraformaldehyde was added. The reaction was allowed to stir for 3 h. Upon completion, the solvent was removed *in vacuo*, and the contents of the round-bottom flask were filtered with benzene to separate from excess paraformaldehyde. The product was recrystallized from cold hexane as an off-white powdery solid (0.060 g, 29% yield): ^{1}H NMR (C_6D_6) δ 0.72 (s, 36 H, Si(CH_3)$_3$), 0.77 (m, 18 H, PCH_2CH_3), 1.42 (m, 6 H, P*C*H_2CH$_3$), 1.71 (m, 6 H, P*C*H_2CH$_3$), 5.65 (d with ^{195}Pt satellites: $^4J_{P-H}$ = 10.0 Hz, $^3J_{Pt-H}$ =

(10) (a) Koe, J. R.; Tobita, H.; Suzuki, T.; Ogino, H. *Organometallics* **1992**, *11*, 150. (b) Koe, J. R.; Tobita, H.; Ogino, H. *Organometallics* **1992**, *11*, 2479. (c) Ogino, H.; Tobita, H. *Adv. Organomet. Chem.* **1998**, *42*, 223.
(11) (a) Litz, K. E.; Henderson, K.; Gourley, R. W.; Banaszak Holl, M. M. *Organometallics* **1995**, *14*, 5008. (b) Litz, K. E.; Bender, J. E.; Kampf, J. W.; Banaszak Holl, M. M. Unpublished results.
(12) Nyman, C. J.; Wymore, C. E.; Wilkinson, G. *J. Chem. Soc. (A)* **1968**, 561.
(13) Hayward, P. J.; Blake, D. M.; Wilkinson, G.; Nyman, C. J. *J. Am. Chem. Soc.* **1970**, *92*, 5873.
(14) Gynane, M. J. S.; Harris, D. H.; Lappert, M. F.; Power, P. P.; Riviere, P.; Riviere-Baudet, M. *J. Chem. Soc., Dalton Trans.* **1977**, 2004.

40.0 Hz); $^{13}C\{^1H\}$ NMR (C_6D_6) δ 7.86 (s, Si(CH_3)$_3$), 8.49 (m, PCH_2CH_3), 8.78 (m, PCH_2CH_3) 14.4 (m, PCH_2CH_3), 19.5 (m, PCH_2-CH_3), 99.3 (br s, Pt−OCH_2); $^{31}P\{^1H\}$ NMR (C_6D_6) δ 19.50 (d with ^{195}Pt satellites: $^2J_{P-P}$ = 14.7 Hz, $^1J_{Pt-P}$ = 1833 Hz), −6.74 (d with ^{195}Pt satellites: $^2J_{P-P}$ = 14.7 Hz, $^1J_{Pt-P}$ = 3494 Hz); IR (Nujol/NaCl) [cm^{-1}, (intensity)] 1251 (vs), 1159 (m), 1110 (m), 1033 (m), 941 (m), 899 (s), 871 (m), 765 (m), 667 (w). Anal. Calcd: C, 33.86; H, 7.73; N, 3.16. Found: C, 33.86; H, 7.55; N, 3.04.

Kinetics of Isomerization of 1 to 2. An evacuated, flame-sealed 5 mm Pyrex NMR tube containing a 0.25 mL of C_6D_6 solution of 0.050 g (0.058 mmol) of **1** was irradiated at a distance of 17 cm from a 100 W Sylvania Par38 mercury lamp at a temperature of 30 °C. Kinetic measurements were obtained at 0, 300, 480, 720, and 960 s intervals by integration of the ^{31}P NMR signal. The final value was monitored at 81% completion. Isomerization was zero order with an observed rate constant of 0.000854 s^{-1} with a least-squares fit to the linear equation $y = 0.000854x + 0.0580$ ($r = 0.998$).

Photolysis of 1 with a Germylene Trap. As above, a benzene-d_6 solution containing 0.050 g of **1** (0.058 mmol) and 10 equiv of benzil (0.120 g, 0.580 mmol) was photolyzed 17 cm from a 100 W Sylvania Par 38 mercury lamp at a temperature of 30 °C. Quantitative conversion to **2** was observed. No evidence of trapped germylene product was detected.

Reduction of 3. A 5 mg (0.005 mmol) amount of **3** was reduced in an excess of sodium/mercury amalgam in THF. After being stirred 1 h, the initially colorless solution became olive-drab in color. THF was removed *in vacuo*. The remaining solids were extracted from the amalgam with C_6D_6 and filtered in the drybox through a Pasteur pipet containing packed glass wool. ^{1}H NMR demonstrated quantitative conversion to $(Et_3P)_2PtGe[N(SiMe_3)_2]_2$. ^{1}H NMR ($C_6D_6$): δ 0.52 (s, 36 H, $SiMe_3$), 1.00 (m, 18 H, PCH_2CH_3), and 1.45 (m, 12 H, PCH_2CH_3); consistent with the previously published data for $(Et_3P)_2PtGe$-$[N(SiMe_3)_2]_2$.

Oxygen-18 Study of the Reaction between 1 and SO_2. Oxygen-18 labeled **1** ($^{18}O_2$-**1**) was prepared according to the procedure given above using 95% $^{18}O_2$ (ICON Services). Oxygen-18 labeled **3** ($^{18}O_2$-**3**) was prepared by addition of unlabeled SO_2 to $^{18}O_2$-**1** in the manner described for the synthesis of **3**. Infrared spectra for **1**, $^{18}O_2$-**1**, **3**, and $^{18}O_2$-**3** were recorded from 4000 to 400 cm^{-1} as KBr pellets and from 600 to 200 cm^{-1} as CsI pellets.

X-ray Crystal Structure Determinations. Table 1 provides a general summary of crystallographic parameters. For structures **1** and **2a**, extensive checks were made to confirm the choice of space group and check for higher symmetry. The metric symmetry was established using the LePage algorithm.[15] A search for additional missing symmetry was performed utilizing subroutines available as part of the PLATON suite of programs (PLATON, Program for the Automated Analysis of Molecular Geometry, A. L. Spek, Utrecht University, The Netherlands, 1997).[16] Neither structure exhibited problems during the refinement (correlations between least-squares parameters, unusually distorted geometries) typical of missing symmetry. Both structures were therefore determined to contain 2 crystallographically independent molecules per asymmetric unit.

$C_{24}H_{66}N_2O_2Si_4P_2GePt$ (1). A colorless crystal of **1** having dimensions 0.42 × 0.32 × 0.26 mm was mounted on a glass fiber with paratone N hydrocarbon oil and placed in a cold stream of nitrogen at 148(2) K. X-ray data collection was performed on a Siemens R3/v automated diffractometer with graphite-monochromatized Mo Kα radiation (λ = 0.710 73 Å) and solved by direct methods with the programs SHELXTL PLUS and SHELXL-93. A 15% decrease in standard intensities was observed and corrected. The data were corrected for absorption using a semiempirial method based on ψ-scans.[17] All non-hydrogen atoms were allowed to refine anisotropically, with hydrogen atoms placed in idealized positions. Additional details: scan method ω, scan rate 10°/min, background-to-scan ratio 0.5, ω scan range 5−45°. The largest peak in the final difference map was 5.750 e Å^{-3} and was associated with Pt.

$C_{24}H_{66}N_2O_2Si_4P_2GePt$ (2a). A colorless crystal having dimensions 1.0 × 0.6 × 0.5 mm was mounted in a flame-sealed glass capillary. X-ray data collection was performed using a Siemens P4 single-crystal diffractometer. Three standard reflections were measured after every 97 reflections; a 16.5% decrease in standard intensities was observed and corrected. Data reduction included profile fitting and a semiempirical absorption correction based on ψ-scans.[17] The structure was determined by Patterson methods. Atoms heavier than carbon were refined with anisotropic displacement parameters. All expected hydrogen atoms were introduced in ideal positions. Final refinement on F^2 was carried out using SHELXL 93.

$C_{26}H_{70}N_2O_{4.5}SSi_4P_2GePt$ (3·0.5THF). A colorless thin, needlelike crystal, having the dimensions 0.06 × 0.24 × 0.46 mm, was mounted in paratone N hydrocarbon oil and placed in a cold nitrogen stream (158(2) K). X-ray data collection was performed on a Siemens SMART diffractometer with a CCD area detector equipped with a normal focus Mo-target X-ray tube (λ = 0.710 73 Å) operated at 2000 W power (50 kV, 40 mA). The frames were integrated with Siemen's SAINT software package with a narrow frame algorithm. All non-hydrogen atoms were allowed to refine anisotropically with hydrogen atoms placed in idealized positions. An absorption correction was applied using SADABS.[18]

$C_{27}H_{66}Cl_6GeN_2O_3P_2PtSi_4$ (4·2CHCl$_3$). X-ray-quality crystals were grown from concentrated chloroform solutions of **4** by slow evaporation of solvent. A small, colorless crystal (dimensions 0.38 × 0.30 × 0.16 mm) was selected, mounted on a glass fiber in paratone N hydrocarbon oil, and placed in a cold stream of nitrogen (153(2) K) on the diffractometer. X-ray data collection was performed on a Siemens SMART diffractometer with a CCD area detector equipped with a normal focus Mo-target X-ray tube (λ = 0.710 73 Å) operated at 2000 W power (50 kV, 40 mA). The frames were integrated with Siemen's SAINT software package with a narrow frame algorithm All non-hydrogen atoms were allowed to refine anisotropically, with hydrogen atoms placed in idealized positions. An absorption correction was applied using SADABS. The largest peak in the final difference map was 5.249 e Å^{-3} and was associated with Pt.

Results

A yellow-orange solution of $(Et_3P)_2PtGe[N(SiMe_3)_2]_2$ was exposed to dioxygen resulting in the rapid formation of a colorless solution. Protection of the reaction from ambient light allowed formation of a new product containing *cis* inequivalent PEt_3 groups as indicated by ^{1}H, ^{13}C, and ^{31}P NMR spectroscopy. The spectroscopic signature of an unsymmetrical, square-planar Pt(II) complex supported assigning this new product as the peroxo complex, $(Et_3P)_2Pt(\mu\text{-}\eta^2\text{-}O_2)Ge[N(SiMe_3)_2]_2$ (**1**). IR spectra of peroxo bimetallic complexes typically show an O−O stretch between 800 and 950 cm^{-1}.[4] However, the assignment of the O−O stretch in **1** was made difficult due to the overlap of strong Ge−N and Si−N stretches in that region. Synthesis of $^{18}O_2$-labeled **1** allowed the observation of a new band at 796 cm^{-1} which has been tentatively assigned as the ^{18}O−^{18}O stretch. To confirm our structural assignment and to examine the impact of the Pt−Ge moiety on O−O activation, an X-ray structure determination of **1** was performed.

X-ray-quality crystals were grown from an ether solution maintained at −10 °C and protected from light (Table 1). The presence of a bridging peroxo moiety spanning a Pt−Ge bond was confirmed (Figure 1). The four-membered ring displays noticeable distortion as indicated by the O−Pt−Ge−O dihedral angle of 13.4°. This puckering of the ring is related to the rotation of the GeN_2 fragment away from a perpendicular orientation to the PtP_2 fragment by 32°. The variation in bond length required in the four-membered ring (Pt1−O1 = 2.050(8)

(15) LePage, Y. J. *J. Appl. Crystallogr.* **1982**, *15*, 225.
(16) Spek, A. L. *Acta Crystallogr.* **1990**, *46A*, C34.
(17) *XEMP, V. 3.43*; Siemens Analytical X-ray Instruments, Inc.: Madison, WI, 1988.
(18) Blessing, R. H. *Acta Crystallogr.* **1995**, *A51*, 33.

Table 1. X-ray Data

compd	**1**	**2a**	**3**	**4**
empirical formula	$C_{24}H_{66}GeN_2O_2P_2PtSi_4$	$C_{24}H_{66}GeN_2O_2P_2PtSi_4$	$C_{24}H_{66}GeN_2O_4P_2PtSSi_4 \cdot 0.5C_4H_8O$	$C_{25}H_{64}GeN_2O_3P_2PtSi_4 \cdot 2CHCl_3$
fw	856.77	856.77	956.88	1121.50
temp	148(2) K	298(2) K	158(2) K	158(2) K
wavelength	0.710 73 Å	0.710 73 Å	0.710 73 Å	0.710 73 Å
cryst system	triclinic	triclinic	monoclinic	monoclinic
space group	$P\bar{1}$ (No. 2)	$P\bar{1}$ (No. 2)	$P2_1/c$ (No. 14)	$P2_1/c$ (No. 14)
unit cell dimens	$a = 11.689(2)$ Å, $\alpha = 108.74(1)°$ $b = 18.753$ (2) Å, $\beta = 97.56(1)°$ $c = 19.160(2)$ Å, $\gamma = 95.44(1)°$	$a = 12.346(3)$ Å, $\alpha = 68.97(2)°$ $b = 17.752(3)$ Å, $\beta = 81.76(2)°$ $c = 20.521(5)$ Å, $\gamma = 74.07(2)°$	$a = 11.6826(1)$ Å $b = 22.6072(2)$ Å, $\beta = 94.5360(10)°$ $c = 17.19130(10)$ Å	$a = 23.904(6)$ Å $b = 11.046(3)$ Å, $\beta = 107.272(13)°$ $c = 19.613(4)$ Å
V, Z	3900.5(9) Å^3, 4	4032(2) Å^3, 4	4526.19(5) Å^3, 4	4946(2) Å^3, 4
abs coeff	4.580 mm^{-1}	4.431 mm^{-1}	4.003 mm^{-1}	3.947 mm^{-1}
$F(000)$	1744	1744	1952	2256
cryst size (mm)	0.42 × 0.32 × 0.26 mm	1.0 × 0.6 × 0.5 mm	0.06 × 0.24 × 0.46 mm	0.38 × 0.30 × 0.16 mm
θ range for data collcn	2.50−22.50°	1.87−25°	2.16−29.42°	2.57−26°
limiting indices	$-12 \le h \le 12$, $-18 \le k \le 18$, $-1 \le l \le 20$	$-1 \le h \le 14$, $-19 \le k \le 19$, $-24 \le l \le 24$	$-15 \le h \le 15$, $-30 \le k \le 29$, $-23 \le l \le 22$	$-29 \le h \le 28$, $-1 \le k \le 13$, $-1 \le l \le 24$
reflcns collcd	10 637	16 039	46 853	12 299
indepdt reflcns	9823	13904 [R(int) = 0.0574]	11512 [R(int) = 0.0339]	9704 [R(int) = 0.0761]
abs corr	ψ-scans	ψ-scans	SADABS	SADABS
max and min transm	1.341and 0.636	0.292 and 0.106	0.915 and 0.614	0.937 and 0.338
refinement method	full-matrix least-squares on F^2	full-matrix least-squares on F^2	full-matrix least-squares on F^2	full-matrix least-squares on F^2
data/restraints/param	9814/0/688	13902/0/409	11492/0/420	9700/0/435
goodness-of-fit on F^2	1.085	0.887	1.092	0.980
final R indices [$I > 2\sigma(I)$]	$R1 = 0.0550$, w$R2 = 0.1421$	$R1 = 0.0633$, w$R2 = 0.1498$	$R1 = 0.0264$, w$R2 = 0.0728$	$R1 = 0.0675$, w$R2 = 0.1693$
R indices (all data)[a]	$R1 = 0.0750$, w$R2 = 0.1488$	$R1 = 0.1263$, w$R2 = 0.1715$	$R1 = 0.0315$, w$R2 = 0.0755$	$R1 = 0.0876$, w$R2 = 0.1755$
extinction coeff	no corr applied	no corr applied	0.000 22(5)	no corr applied
largest diff peak and hole	5.750 and −2.520 e Å^{-3}	1.054 and −1.710 e Å^{-3}	1.563 and −0.998 e Å^{-3}	5.249 and −3.430 e Å^{-3}
diffractometer	Siemens P4U, equipped with LT-2	Siemens P4	Siemens SMART-CCD /LT-2	Siemens P4U, equipped with LT-2

[a] $R1 = \sum(|F_o| - |F_c|)/\sum|F_o|$; $wR2 = [\sum w(F_o^2 - F_c^2)/\sum w(F_o^2)^2]^{1/2}$.

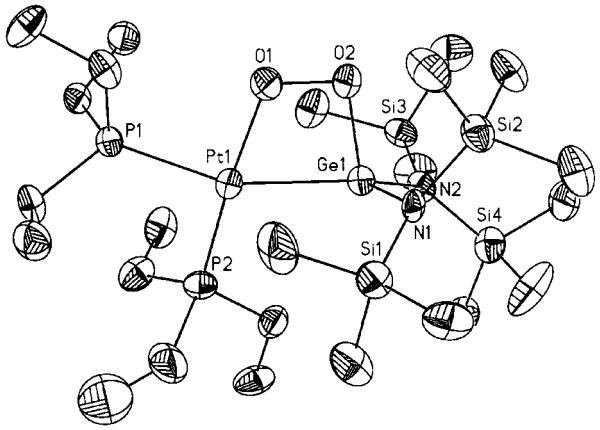

Figure 1. ORTEP of **1** (50% probability). Selected bond lengths (Å) and angles (deg) are reported for one of the two independent molecules in the unit cell. No chemically significant deviations were noted: Pt1−P1 = 2.318(3); Pt1−P2 = 2.219(3); Pt1−O1 = 2.050(8); O1−O2 = 1.503(11); O2−Ge1 = 1.847(8); Ge1−N1 = 1.847(8); Ge1−N2 = 1.888(8); Pt1−Ge1 = 2.4286(13); P1−Pt1−P2 = 96.17(11); P2−Pt1−Ge1 = 107.79(9); P1−Pt1−Ge1 = 156.00(8); P1−Pt1−O1 = 88.5(2); O1−Pt1−Ge1 = 67.8(2); Pt1−O1−O2 = 107.0(5); O1−O2−Ge1 = 96.9(5); O2−Ge1−Pt1 = 83.3(2); N1−Ge1−N2 = 110.2(4); N1−Ge1−Pt1 = 119.9(3); N2−Ge1−Pt1 = 126.8(3); O2−Ge1−N1 = 102.4(4); O2−Ge1−N2 = 103.1(4).

Scheme 1. Complete Reaction Cycle Showing Formation of Bridging Peroxide, Oxidation of SO_2, and Reduction of Sulfate To Yield Starting Complex with Photochemical Isomerization of the Peroxide to a Germanate Moiety Also Shown

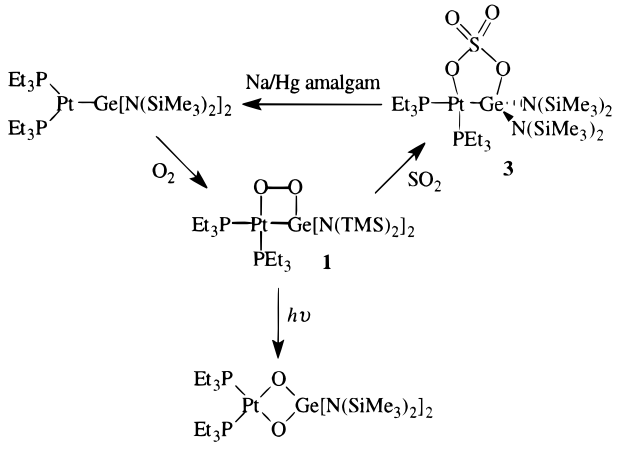

Å; Pt1−Ge1 = 2.4286(13) Å; O1−O2 = 1.503(11) Å; Ge1−O1 = 1.847(8) Å) probably drives this distortion as steric crowding of the triethylphosphine and (trimethylsilyl)amide groups does not appear to be a limiting factor on the basis of a comparison with the structures of the three-coordinate metal germylene complexes and other metallocycles.[11a,19] As has been typical for the four-membered metallacyles synthesized in this system to date, the coordination geometry about germanium can best be described as a distorted trigonal pyramidal with the base formed by Pt and two N atoms and the cap formed by oxygen. The O−O bond distance is somewhat shorter than that observed by Cowie et al. in the iridium system (1.58(2) Å) and that observed by Bhaduri et al. in $[Ph_3P)_2Pt(\mu\text{-}O_2)(\mu\text{-}OH)]_2ClO_4$ (1.547(21) Å).[20] The distance observed in **1** is within one

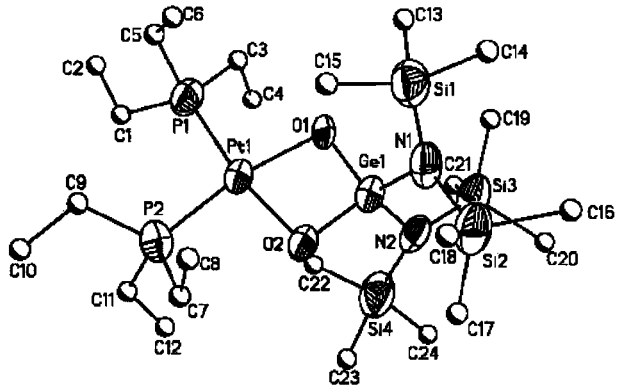

Figure 2. ORTEP of **2a** (50% probability). Selected bond lengths (Å) and angles (deg) are reported for one of the two independent molecules in the unit cell. No chemically significant deviations were noted: Pt1−O1 = 2.070(6); Pt1−O2 = 2.032(8); Pt1−P1 = 2.226(3); Pt1−P2 = 2.224(3); Ge1−O1 = 1.738(8); Ge1−O2 = 1.784(7); Pt1−Ge1 = 2.770(2); Ge1−N1 = 1.841(10); Ge1−N2 = 1.861(9); O2−Pt1−O1 = 78.9(3); O2−Pt1−P2 = 89.4(2); O1−Pt1−P2 = 168.2(2) O2−Pt1−P1 = 169.4(2); O1−Pt1−P1 = 90.5(2); P2−Pt1−P1 = 101.29(14); Pt1−O1−Ge1 = 92.9(3); Pt1−O2−Ge1 = 92.8(3); O1−Ge1−O2 = 95.4(3); N1−Ge1−N2 = 111.3(4); N1−Ge1−O1 = 111.3(4); N2−Ge1−O1 = 112.7(4); N2−Ge1−O2 = 112.4(4); N1−Ge1−O2 = 112.9(4).

standard deviation of the mean O−O bond length (1.45(7) Å) for peroxides bridging between two metal centers. The Pt−Ge distance of 2.4286(13) Å falls exactly in the range previously observed for a number of Pt−germyl complexes.[11a,19]

When the reaction of $(Et_3P)_2PtGe[N(SiMe_3)_2]_2$ with O_2 was performed in the presence of ambient light or when crystals of **1** were stored in ambient light, a slow conversion to a complex having symmetrically equivalent triethylphosphine ligands occurred. This conversion was not observed to occur when **1** was protected from light, even upon heating benzene solutions to 80 °C. However, upon exposure of the solutions to UV-light, rapid and quantitative conversion to $(Et_3P)_2PtO_2Ge[N(SiMe_3)_2]_2$ (**2a**) resulted (Scheme 1). Structural assignment of **2a** was based upon spectroscopic data and elemental analysis which indicated the same molecular composition as **1**. A germyl moiety and cis-ligated equivalent triethylphosphines bound to a square-planar platinum(II) center were indicated by ^1H, ^{13}C, and ^{31}P NMR analysis. By analogy to the photochemistry observed for peroxo complexes of disilenes and digermenes,[8,9] it was hypothesized that a similar rearrangement could have taken place to form a Pt(II) germanate complex. This assignment was confirmed by X-ray crystallographic analysis (Figure 2, Table 1). The four-membered ring in **2a** displays considerably less distortion than that found in **1** as evidenced by the nearly planar 0.53(3)° O−Pt−O−Ge dihedral angle. The coordination sphere at germanium remains four-coordinate but changes from the esoteric trigonal-pyramidal geometry to a more common tetrahedral coordination polyhedra formed by two oxygen atoms and two nitrogen atoms. Coordination about the Pt center is roughly square-planar. The largest deviation is found in the O(1)−Pt−O(2) angle of 78.9(3)°. Like similarly bonded silicon complexes, the metals on opposite corners of the square are held in rather close proximity to each other. The Pt−Ge distance of 2.770(2) Å is 0.34 Å longer than that observed for the platinum−germyl bond in complex **1**. By way of comparison, the Ge−Ge bond length the cyclodigermoxane synthesized by Masamune et al. was found to be 2.617(1) Å, about 0.16 Å

(19) Litz, K. E.; Kampf, J. W.; Banaszak Holl, M. M. *J. Am. Chem. Soc.* **1998**, *120*, 7484.

(20) Bhaduri, S.; Casella, L.; Ugo, R.; Raithby, P. R.; Zuccaro, C.; Hursthouse, M. B. *J. Chem. Soc., Dalton Trans.* **1979**, 1624.

longer than a typical Ge−Ge bond.[8] Both of these germanium containing rings contrast sharply with the observation of West et al. that four-membered ring cyclosiloxanes have closer than expected Si−Si distances.[21]

The reaction of $(Ph_3P)_2PtO_2$ and $Ge[N(SiMe_3)_2]_2$ was examined to determine if a peroxo complex or germanate complex would form. The reaction was protected from light to prevent degradation of a peroxo complex. Germanate complex **2b** was assigned as the sole product of this reaction (eq 3). ^1H, ^{13}C,

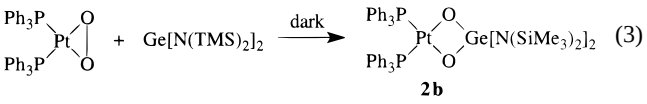

(3)

and ^{31}P NMR spectra revealed the complex to possess *cis*-equivalent triphenylphosphine ligation to a Pt(II) center. Direct formation of **2b** suggested that isomerization from **1** to **2a** may proceed via ejection of germylene and subsequent recombination of $(Et_3P)_2PtO_2$ and $Ge[N(SiMe_3)_2]_2$ to form **2a**. Another alternative mechanism involving the photodissociation of the metallacycle into O_2 and $(Et_3P)_2PtGe[N(SiMe_3)_2]_2$, followed by photolytic dissociation of germylene, formation of $(Et_3P)_2PtO_2$, and subsequent reaction to form **2a**, was also considered on the basis of the analogy to results previously observed for $(Et_3P)_2Pt(\mu\text{-}\eta^2\text{-}H_2CO)Ge[N(SiMe_3)_2]_2$.[11b] To test for the presence of free germylene during the isomerization of **1** to **2a**, chemical trapping experiments were performed. Photolysis of **1** with 10 equiv of benzil, an efficient germylene trap,[11b,22] gave no evidence of free germylene during the isomerization of **1** to **2a**. The rate of isomerization was measured for a 0.058 mmol solution of **1** in C_6D_6 exposed to a 100 W SylvaniaPar 38 mercury lamp. A rate constant of 0.00085 s^{-1} was obtained, and the reaction was found to be zero order with respect to metal concentration. Taken together, the kinetic data and the fact that free germylene is not generated during the isomerization suggest an intramolecular conversion from **1** to **2a**.

The chemical behavior of the unique peroxo bridging found in **1** was tested with a variety of reagents. Unlike many type II peroxo complexes of Ni, Pd, and Pt, **1** did not react with CO_2, ketones, alkenes, alkynes, or alkyl- and arylphosphines.[4,23] The lack of reactivity cannot be explained solely as a steric effect because reagents such as CO_2 were observed to react with the more sterically bulky nitrosobenzene adduct.[19] Instead, these observations imply an electronically based selectivity that differs between type II Pt peroxo complexes and the type X peroxo complex reported here. Two reagents were observed to react with **1**, SO_2 and $H_2C{=}O$, and the results from these reactions are presented below.

Reaction of excess SO_2 with a benzene solution of **1** resulted in the rapid formation of an insoluble solid. Characterization of the white precipitate by ^1H, ^{13}C, and ^{31}P NMR spectroscopy revealed quantitative conversion of **1** to a new complex possessing *cis*-inequivalent triethylphosphines and a germyl moiety coordinated to platinum in a square planar fashion. IR spectroscopy revealed the presence of strong S=O stretches indicative of a sulfate group at 1279 and 1159 cm^{-1}. On the basis of spectroscopic analysis, the structure was assigned as the bridging sulfate complex, $(Et_3P)_2Pt(\mu\text{-}\eta^2\text{-}SO_4)Ge[N(SiMe_3)_2]_2$ (**3**) (Scheme 1). An X-ray crystallographic analysis was performed to confirm this assignment (Figure 3, Table 1).

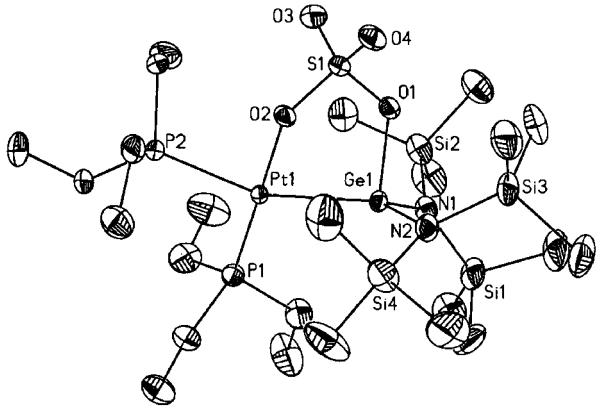

Figure 3. ORTEP of **3** (50% probability). Bond lengths (Å) and angles (deg): Pt1−Ge1 = 2.4663(3); Pt1−P1 = 2.2271(8); Pt1−P2 = 2.3374(8); Pt1−O2 = 2.096(2); Ge1−O1 = 1.911(2); Ge1−N1 = 1.875(3); Ge1−N2 = 1.869(3); S1−O1 = 1.538(2); S1−O2 = 1.517(2); S1−O3 = 1.443(3); S1−O4 = 1.442(3); P1−Pt1−P2 = 98.76(3); P1−Pt1−O2 = 175.84(7); P2−Pt1−O2 = 80.90(6); Ge1−Pt1−P1 = 103.46(2); Ge1−Pt1−P2 = 157.65(2); N1−Ge1−N2 = 112.01(13); N2−Ge1−O1 = 98.80(11); N1−Ge1−O1 = 95.77(12); N2−Ge1−Pt1 = 119.65(9); N1−Ge1−Pt1 = 125.36(9); O1−Ge1−Pt1 = 93.02(7); O2−Pt1−Ge1 = 77.12(6); O2−S1−O1 = 105.02(12); Pt1−O2−S1 = 122.56(13); S1−O1−Ge1 = 118.4(13); O3−S1−O4 = 114.8(2); O2−S1−O4 = 108.58(14); O2−S1−O3 = 110.5(2); O1−S1−O4 = 109.24(14); O1−S1−O3 = 108.32(14).

The five-membered ring formed by Pt−O−S−O−Ge atoms represents the most prominent structural feature of **3**. The dihedral angle formed by the O−Pt−Ge−O portion of this ring is 35.08(9)°. The Pt−O distance of 2.096(2) Å is longer than observed for complexes **1** or **2a** (2.050(8); 2.070(6), 2.032(8) Å). The Ge−O bond length of 1.911(2) Å is also longer than those observed for **1** or **2a** (1.847(8); 1.738(8), 1.784(7) Å) and longer than that seen in the previously characterized complexes $(Et_3P)_2Pt(\mu\text{-}\eta^2\text{-}CO_2)Ge[N(SiMe_3)_2]_2$ (1.883(5) Å) and $(Et_3P)_2Pt(\mu\text{-}\eta^2\text{-}PhNO)Ge[N(SiMe_3)_2]_2$ (1.820(4) Å).[11a,19] The sulfate shows significant deviation in the S−O bond lengths (1.538(2), 1.517(2), 1.443(3), 1.442(3) Å) as compared to "free" sulfate ions which typically show distances in the 1.46−1.48 Å range. Similar changes in bond length have been observed previously for sulfate bridging across two platinum centers.[24] The coordination sphere about germanium resembles a distorted trigonal pyramid, and the coordination about platinum is roughly square-planar.

Given the general difficulty in designing catalytic conversions of SO_2 to $[SO_4]^{2-}$,[5] we were interested in the feasibility of removing the sulfate fragment from **3** to regenerate $(Et_3P)_2PtGe[N(SiMe_3)_2]_2$. Unlike Cowie's peroxo complex, **3** is well suited for simple reduction reactions as there are no halide ligands to cause potential side reactions. Reduction of **3** in THF solution with Na/Hg amalgam quantitatively removed the sulfate moiety and quantitatively regenerated $(Et_3P)_2PtGe[N(SiMe_3)_2]_2$ as demonstrated by ^1H NMR spectroscopy (Scheme 1). To better understand the interaction of strongly coordinating anions such as sulfate with the metal−germylene complexes, we synthesized a carbonate complex. Addition of 1 equiv of $Ge[N(SiMe_3)_2]_2$

(21) Fink, M. J.; Haller, K. J.; West, R.; Michl, J. *J. Am. Chem. Soc.* **1984**, *106*, 822.

(22) (a) Tokitoh, N.; Manmura, K.; Okazaki, R. *Organometallics* **1994**, *13*, 167. (b) Weidenbruch, M.; Stürmann, M.; Kilian, H.; Pohl, S.; Saak, W. *Chem. Ber. Recueil* **1997**, *130*, 735.

(23) (a) Nyman, C. J.; Wilkinson, G. *J. Chem. Soc., Chem. Commun.* **1967**, 407. (b) Hayward, P. J.; Blake, D. M.; Nyman, C. J.; Wilkinson, G. *J. Chem. Soc., Chem. Commun.* **1969**, 987. (c) Otsuka, S.; Nakamura, A.; Tatsuno, Y.; Miki, M. *J. Am. Chem. Soc.* **1972**, *94*, 3761.

(24) (a) Cotton, F. A.; Falvello, L. R.; Han, S. *Inorg. Chem.* **1982**, *21*, 2889. (b) Zhilyaev, A. N.; Shikhaleeva, E. V.; Katsen, S. B.; Baranovsky, I. B. *Zh. Neorg. Khim.* **1987**, *32*, 118.

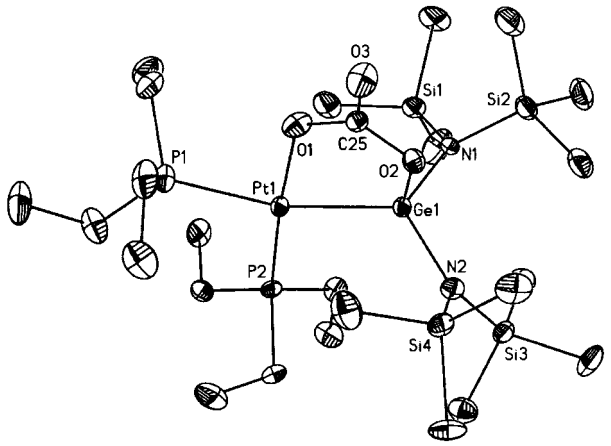

Figure 4. ORTEP of **4** (50% probability). Selected bond lengths (Å) and angles (deg): Pt1−Ge1 = 2.4174(10); Pt1−P1 = 2.355(2); Pt1−P2 = 2.229(2); Pt1−O1 = 2.091(6); Ge1−O2 = 1.864(6); C25−O1 = 1.319(10); C25−O2 = 1.337(10); C25−O3 = 1.249(10); Ge1−N1 = 1.868(8); Ge1−N2 = 1.889(8); P1−Pt1−P2 = 104.52(9); N1−Ge1−N2 = 113.7(3); P1−Pt1−O1 = 79.8(2); P2−Pt1−O1 = 174.6(2); P2−Pt1−Ge1 = 96.07(7); P1−Pt1−Ge1 = 158.96; Pt1−O1−C25 = 121.4(5); O1−C25−O2 = 120.5(7); O1−C25−O3 = 120.3(8); O3−C25−O2 = 119.2(8); C25−O2−Ge1 = 116.5; O2−Ge1−Pt1 = 95.0(2); O2−Ge1−N1 = 98.6(3); O2−Ge1−N2 = 95.6(3).

to a solution of $(Et_3P)_2PtCO_3$ in THF resulted in insertion of the germylene into the Pt−O bond and formation of $(Et_3P)_2$-Pt(μ-η^2-OC(O)O)Ge[N(SiMe$_3$)$_2$]$_2$ (**4**) (eq 4). Characterization

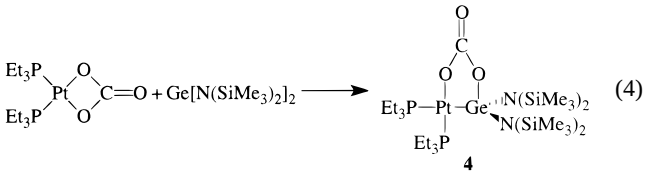

(4)

4

by ^{1}H, ^{13}C, and ^{31}P NMR spectroscopy indicated a square-planar complex with *cis*-inequivalent triethylphosphine ligands. A single-crystal X-ray diffraction study confirmed the overall geometry and provided important metrical parameters for comparison to sulfate complex **3** (Figure 4). The five-membered ring contains a planar CO_3 fragment and possesses a 19.98° OPtGeO dihedral angle. The Pt−O and Ge−O bond lengths are 2.091(6) and 1.864(6) Å, respectively, and the carbonate C−O distances are 1.319(10), 1.337(10), and 1.249(10) Å. Note that the C25−O1 and C25−O2 bond lengths are significantly longer and C25−O3 is significantly shorter than those previous observed for similar bridging carbonates.[25] This suggests that the carbonate in complex **4** lies the farthest along the continuum toward formal single bonds and a double bond for the carbon−oxygen interaction. In concert with the Ge−O bond length, these structural parameters suggest that the carbonate is more strongly bound than the sulfate. By way of contrast, the 1.911(2) Å Ge−O bond length of the sulfate is one of the longest observed, exceeded only by a trichloromethyl acetate bridged dimer of tetraphenyldigermane (2.073(3) and 2.314(3) Å)[26] and a trifluoromethanesulfonate-stabilized diphenylgermylene ligand in a rhenium complex (2.034(4) Å).[27] To date, 90% of crystallographically characterized Ge−O bonds lengths in molecular species have been observed between 1.73 and 1.83 Å. The Pt−O bonds of **3** and **4** are both longer than the mean length observed for square-planar platinum complexes (2.05(4) Å). Attempts at reducing the carbonate complex to generate $(Et_3P)_2$PtGe-[N(SiMe$_3$)$_2$]$_2$ failed. Reduction with Na/Hg amalgam did not result in any reaction, and reduction with cesium attacked the bis(trimethylsilyl)amide groups on the germylene. The reaction of **1** with CO did not provide an alternate route to **4**.

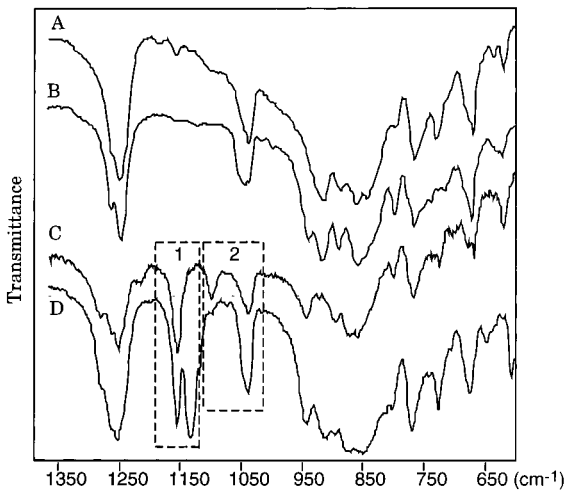

Figure 5. Infrared spectra of **1** (A), $^{18}O_2$-**1** (B), **3** (C), and $^{18}O_2$-**3** (D) (KBr pellets) from 1350 to 550 cm^{-1}.

The formation of sulfate complex **3** was studied by infrared spectroscopy by comparison of isotopically labeled and unlabeled compounds. $^{18}O_2$-**1** was prepared by addition of $^{18}O_2$ (95% ^{18}O) to $(Et_3P)_2$PtGe[N(SiMe$_3$)$_2$]$_2$. Addition of unlabeled SO_2 to $^{18}O_2$-**1** resulted in the partially labeled sulfate complex, $^{18}O_2$-**3**. The symmetric S=O stretch in **3** appears at 1159 cm^{-1} (Figure 5C, region 1). The asymmetric S=O stretch is obscured by the strong Si(CH$_3$)$_3$ deformations at 1251 cm^{-1}. The partially labeled sulfate complex possesses two symmetric S=O stretches of roughly equal intensity at 1152 and 1131 cm^{-1} (calculated shift = 1114 cm^{-1}) indicating label incorporation at a single external S=O site (Figure 5D, region 1). In addition, the Ge−O stretch at 1096 cm^{-1} in **3** shifts to 1040 cm^{-1} in $^{18}O_2$-**3** indicative of no exchange at the Ge−O bond (Figure 5, region 2). The infrared spectra of **1** and $^{18}O_2$-**1** between 1300 and 550 cm^{-1} were identical with the exception of an as yet unassigned absorbance at 934 cm^{-1} in $^{18}O_2$-**1** and the ^{18}O−^{18}O stretch tentatively assigned at 796 cm^{-1} (Figure 5A,B). In the infrared region between 600 and 200 cm^{-1}, Pt−O stretches are reported to occur near 400 cm^{-1}.[28] Unlabeled **1** possessed a broad absorption in this region centered at 417 cm^{-1} (Figure 6A). Comparison to $^{18}O_2$-**1** reveals a band shifted as predicted by harmonic oscillator approximation at 402 cm^{-1} (Figure 6B). Therefore we assigned the peak at 417 cm^{-1} as a Pt−O stretch. The other absorptions observed likely result from ring modes, also known to occur in this region. The IR spectrum of **3**, shown in Figure 6C, was noted to have a broad absorption with a shoulder at 419 and 411 cm^{-1}, assigned as Pt−O modes. The partially labeled sulfate complex, $^{18}O_2$-**3**, also contained a Pt−O stretch at 416 cm^{-1}. Since the peak at 416 cm^{-1} was unshifted, this suggests that the Pt−^{18}O bond is cleaved and an unlabeled O-atom from SO_2 is incorporated.

Insertion of formaldehyde into the Pt−O bond of **1** was also pursued. A THF solution of **1** was generated *in situ* followed

(25) (a) Reinking, M. K.; Ni, J.; Fanwick, P. E.; Kubiak, C. P. *J. Am. Chem. Soc.* **1989**, *111*, 6459. (b) Cotton, F. A.; Labella, L.; Shang, M. Y. *Inorg. Chim. Acta* **1992**, *197*, 149.

(26) Simon, D.; Haberle, K.; Drager, M. *J. Organomet. Chem.* **1984**, *267*, 133.

(27) Lee, K. F.; Arif, A. M.; Gladysz, J. A. *Organometallics* **1991**, *10*, 751.

(28) Socrates, G. *Infrared Characteristic Group Frequencies*; John Wiley and Sons: New York, 1992.

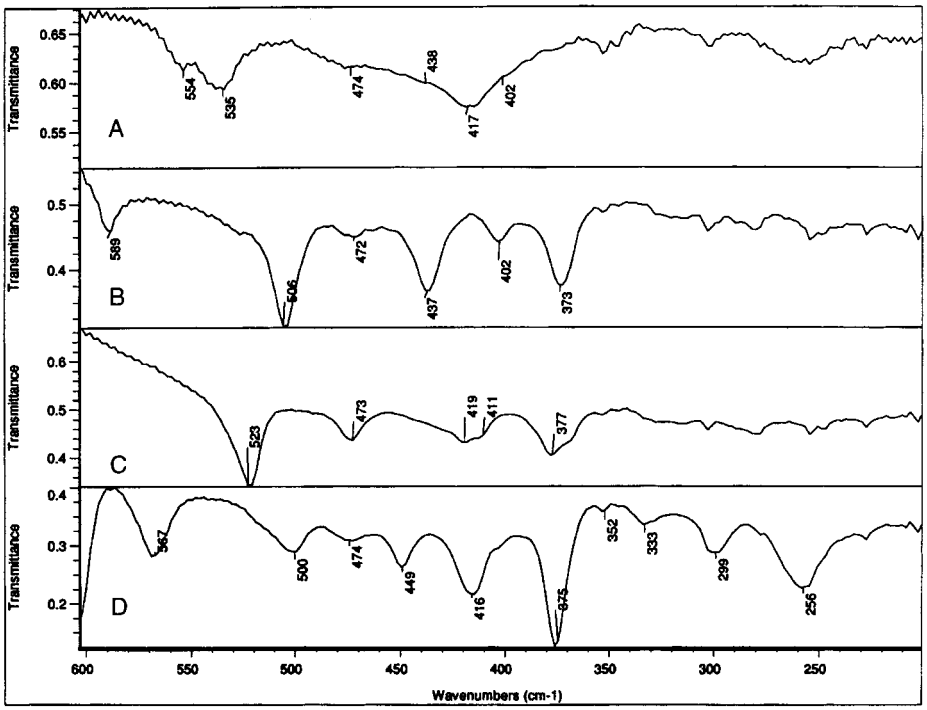

Figure 6. Infrared spectra of **1** (A), $^{18}O_2$-**1** (B), **3** (C), and $^{18}O_2$-**3** (D) (CsI pellets) from 600 to 200 cm^{-1}.

by addition of paraformaldehyde. A new doublet with Pt satellites was observed in the ^{1}H NMR at 5.65 ppm, consistent with the insertion of a formaldehyde unit into the Pt−O bond. The magnitude of the coupling constants ($^4J_{P-H}$ = 10.0 Hz, $^3J_{Pt-H}$ = 40.0 Hz) indicated that the formaldehyde oxygen was bound to platinum. The ^{13}C NMR spectrum showed no discernible Pt coupling for the formaldehyde-derived methylene at 99.3 ppm. The remainder of the spectral data, including ^{31}P NMR spectra and IR spectra, support assignment of the complex as $(Et_3P)_2Pt(\mu\text{-}\eta^2\text{-}OCH_2OO)Ge[N(SiMe_3)_2]_2$ (**5**) (eq 5). This

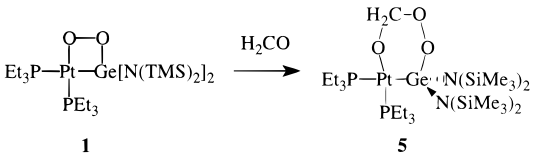

(5)

orientation of insertion is consistent with the previously observed result for the reaction of formaldehyde with $(Et_3P)_2Pt(\mu\text{-}\eta^2\text{-}N(Ph)O)Ge[N(SiMe_3)_2]_2$ which gave $(Et_3P)_2Pt(\mu\text{-}\eta^2\text{-}OCH_2N(Ph)O)Ge[N(SiMe_3)_2]_2$. In this case, the orientation of formaldehyde insertion was confirmed using X-ray crystallography.[19]

Discussion

Reaction of O_2 with $(Et_3P)_2PtGe[N(SiMe_3)_2]_2$ forms peroxide product **1** if the reagents are protected from light. The reactivity observed for **1** indicates this structural hybrid between the main group peroxodigermanes and the peroxoiridium dimer prepared by Cowie et al. (eq 2) can undergo transformations typical to both classes of compounds. **1** photoisomerizes to **2a** in a fashion analogous to the main group bridging peroxides yet also undergoes Pt−O bond insertion chemistry typically observed for transition metal peroxides. This behavior contrasts with that of Cowie's peroxo complex which was observed to decompose upon photoirradiation but underwent insertion reactions with a wider variety of substrates.[7]

Direct synthesis of bidentate, dianionic germanates, such as found in **2a**, is possible via reaction of germylenes with type II peroxide complexes. This was firmly established by addition of $(Ph_3P)_2PtO_2$ to $Ge[N(SiMe_3)_2]_2$, producing the germanate analogue **2b**. Direct synthesis of **2b** raises some interesting issues about complexes **1** and **2a**. The reaction of O_2 with $(Et_3P)_2PtGe[N(SiMe_3)_2]_2$ must occur with the intact Pt−Ge bond. If predissociation of germylene occurred followed by formation of the type II platinum peroxo, complex **2a** would be generated instead of complex **1**. Predissociation of germylene can also be excluded because none was trapped by excess benzil present during the isomerization from **1** to **2a**. Eliminating the presence of free germylene in the process is important because we have recently observed the UV-photolysis of $(Et_3P)_2Pt(\mu\text{-}\eta^2\text{-}H_2CO)Ge[N(SiMe_3)_2]_2$.[11b] Upon irradiation, the bridging formaldehyde moiety undergoes a photocycloreversion reaction at the four-membered ring generating $(Et_3P)_2PtGe[N(SiMe_3)_2]_2$ and formaldehyde. Continued photolysis cleaves the Pt−Ge bond of $(Et_3P)_2PtGe[N(SiMe_3)_2]_2$ to give $(Et_3P)_2Pt$ and free germylene. The $(Et_3P)_2Pt$ fragment causes the decarbonylation reaction of the formaldehyde. The free germylene formed by this photochemical reaction is readily trapped by benzil. Therefore, mechanisms involving cycloreversion of **1**, followed by loss of germylene, and formation of a type II peroxo are inconsistent. The formation of **2a** from **1** likely involves cleavage of the O−O bond by light, rotation, and subsequent formation of the additional Pt−O and Ge−O bonds.

Given the similarity of **1** to $(Ph_3P)_2PtO_2$, comparison of the closely related binding modes and reactivity is informative. In particular, does the change in dioxygen coordination alter the mechanism by which the sulfate reaction proceeds? Mechanistic studies of the reaction of SO_2 with $(Ph_3P)_2PtO_2$ argue for a peroxysulfite or peroxysulfuryl intermediate which rearranges to yield the bidentate sulfate product (Scheme 2).[29] Insertion into the Pt−O bond, instead of direct attack at the O−O bond, is believed to occur because the isotopic label ends up in both the terminal and metal-bound positions of the sulfate. Mehandru

(29) (a) Horn, R. W.; Weissberger, E.; Collman, J. P. *Inorg. Chem.* **1970**, *9*, 2367. (b) Valentine, J.; Valentine, D.; Collman, J. P. *Inorg. Chem.* **1971**, *10*, 219.

Scheme 2. Mechanism of Sulfate Formation in Type II and Type X Peroxides with Spectator Ligands Not Shown

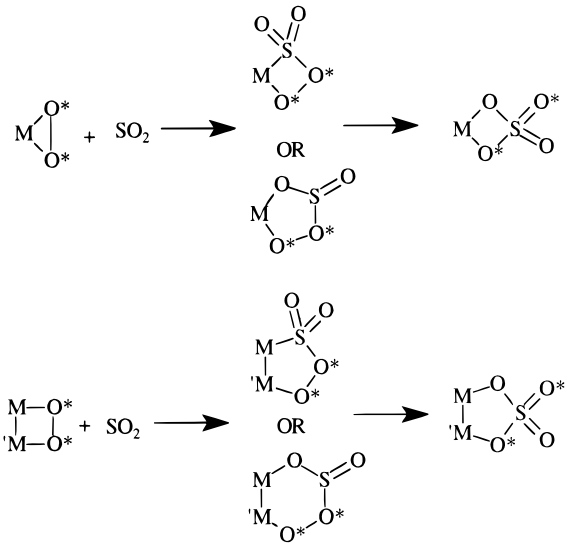

and Anderson studied the mechanism of this reaction theoretically and concluded the five-membered peroxysulfite intermediate was more likely than the four-membered peroxysulfuryl intermediate.[30] They based this conclusion on the high-energy transition state they predicted for conversion of the peroxysulfuryl intermediate to the sulfate. Although the peroxysulfite intermediate was calculated to be less stable, the lower-energy transition state for conversion to sulfate was deemed the more important factor.

The labeling study presented in this paper for the reaction of **1** and SO_2 to form sulfate complex **3** demonstrates this type of bridging peroxide follows the same general mechanism previously proposed by Collman et al. wherein SO_2 inserts into the Pt−O bond and rearranges to the sulfate complex.[29] The oxygen in the Pt−O−S linkage in sulfate complex **3** comes from SO_2, as no shift in the Pt−O region was observed when comparing **3** to $^{18}O_2$-**3**. The IR spectrum of $^{8}O_2$-**3** contains a feature at 1159 cm^{-1}, consistent with a S═^{16}O stretch, and a feature at 1131 cm^{-1}, consistent with a S═^{18}O stretch. The new sulfate S═O stretch at 1131 cm^{-1} at roughly equal intensity to that at 1159 cm^{-1} results from essentially complete transfer of the Pt bound ^{18}O in the initial peroxide complex to an external S═O in **3**. These results indicate type X peroxides undergo the sulfate reaction in a fashion similar to type II peroxides. Both this work and the previous work by Collman et al. definitively excludes

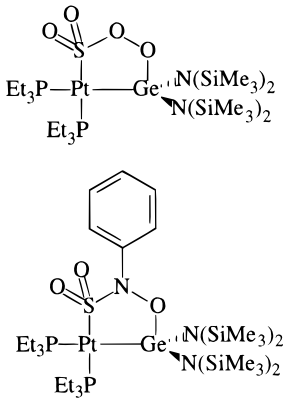

Figure 7. Proposed intermediate for SO_2 insertion into **1**.

direct insertion into the O−O bond of the peroxide as the mechanism for sulfate formation. Unfortunately, neither experimental study has been able to distinguish between a peroxysulfite or peroxysulfuryl intermediate. Although we have been unable to detect any intermediates in the conversion of **1** to **3**, we have isolated and structurally characterized an isoelectronic insertion product for the reaction of SO_2 with $(Et_3P)_2Pt(\mu\text{-}\eta^2\text{-PhNO})Ge[N(SiMe_3)_2]_2$.[19] This analogy suggests that the five-membered ring structure depicted in Figure 7 may be the intermediate for SO_2 insertion into bimetallic peroxo **1**.

We were able to demonstrate removal of the sulfate moiety of **3** by reduction with Na/Hg amalgam. The initial metal starting material, $(Et_3P)_2PtGe[N(SiMe_3)_2]_2$, is regenerated in quantitative yield. As Kubas has noted, the removal of sulfate and regeneration of starting materials has been problematic in designing catalytic conversions of SO_2 to $[SO_4]^{2-}$.[5] The sulfate analogue prepared by addition of SO_2 to Cowie's peroxo−Ir dimer is unsuitable for such a reduction strategy due to the presence of iodide ligands. Although **1** is not an attractive candidate for the catalytic abatement of SO_2, it serves to illustrate the efficacy of strategies that employ reversible Ge−O bond formation and Pt−Ge centers as catalytic sites.

Acknowledgment. Alfa-Aesar is thanked for a loan of K_2PtCl_4. M.M.B.H. thanks the University of Michigan for support of this work and D. Coucouvanis for helpful discussions.

Supporting Information Available: Tables of data collection and refinement parameters, atomic coordinates and thermal parameters including hydrogens, complete bond distances and angles, and anisotropic displacement parameters (35 pages). X-ray crystallographic data files for **1**, **2a**, **3**, and **4**, in CIF format, are available on the Internet only. Ordering and access information is given on any current masthead page.

(30) Mehandru, S. P.; Anderson, A. B. *Inorg. Chem.* **1985**, *24*, 2570.

IC9808044